

RESEARCH ARTICLE

Tailoring PDC speckle structure

G.Brida^a, A.Meda^a, M.Genovese^{a*}, E. Predazzi^b and I.Ruo-Berchera^a

^a*Istituto Nazionale di Ricerca Metrologica, I-10135 Torino, Italia*

^b*Dipartimento di Fisica Teorica Università di Torino and INFN, I-10125 Torino, Italia*

(xx/xx/xxxx)

Speckle structure of parametric down conversion light has recently received a large attention due to relevance in view of applications to quantum imaging

The possibility of tailoring the speckle size by acting on the pump properties is an interesting tool for the applications to quantum imaging and in particular to the detection of weak object under shot-noise limit.

Here we present a systematic detailed experimental study of the speckle structure produced in type II PDC with particular attention to its variation with pump beam properties.

Keywords: parametric down conversion, entanglement, speckles, quantum imaging, quantum correlations

1. Introduction

Thermal or pseudothermal light (as the one obtained by scattering of coherent light by a diffuser) presents a random intensity distribution known as speckle pattern (*las*). This structure can have interesting applications, e.g. in metrology (*uto*).

In particular, speckle structure of parametric down conversion (PDC) light has recently received a large attention due to relevance in view of applications to quantum imaging (*qi*).

The aim of Sub Shot Noise (SSN) quantum imaging is to obtain the image of a weak absorbing object with a level of noise below the minimum threshold that is unavoidable in the classical framework of light detection. Being interested in measuring an image, one is forced to consider a multi-mode source which is able to display quantum correlation also in the spatial domain. Theoretically, this goal can be achieved by exploiting the quantum correlation in the photon number between symmetrical modes of SPDC . Typically the far field emission is collected by a high quantum efficiency CCD camera. It is fundamental to set the dimension of the modes coherence areas with respect to the dimension of the pixels. In particular, the single pixel dimension must be of the same order of magnitude of the coherence area or bigger, in order to fulfill the sub-shot noise correlation condition, compatibly with the requirement of large photon number operation. Thus, the possibility of tailoring the speckle size by acting on the intensity and size of the pump beam represents an interesting tool for the applications to quantum imaging and in particular to the detection of weak objects under shot-noise limit (*qi, lug2, dit, and*).

*Corresponding author. Email: m.genovese@inrim.it

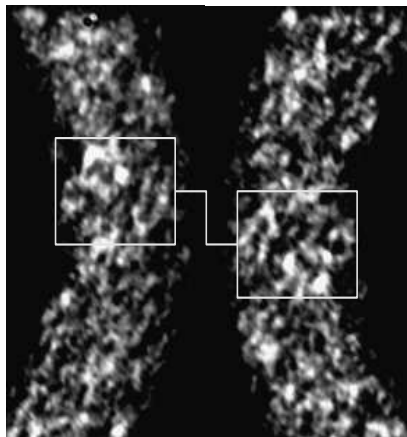


Figure 1. The speckled structure of the light emission from a type II BBO non-linear crystal. The two partial rings represent the two correlated beams 1 and 2, when a filtering of 10 nm around the degeneracy frequency ($\omega_1 = \omega_2 = \omega_p/2$) is applied to the scattered light. Correlated areas can be easily identified.

A detailed theory of correlations and speckle structure in PDC has been developed in (*lug*) and, in another regime, in (*mat*). Furthermore, experimental results were presented in (*dit*).

Nevertheless, a systematic comparison of experimental variation of speckle size and their correlations with the theoretical results of (*lug*) is still missing.

In this paper we present a systematic detailed experimental study of the speckle structure produced in type II PDC with particular attention to its variation with pump beam properties. In particular dependence on pump power and size are investigated in detail.

2. Theory

The process of SPDC is particularly suitable for studying the spatial quantum correlations (*1*), because it takes place with a large bandwidth in the spatial frequency domain. Any pair of transverse modes of the radiation, characterized by two opposite transverse momenta \mathbf{q} and $-\mathbf{q}$, are correlated in the photon number, i.e. they contain, in an ideal situation, the same number of photons. In the far field zone, the single transverse mode is characterized by a coherence area, namely the uncertainty on the emission angle ϑ ($\tan \vartheta = \lambda q/2\pi$, λ being the wavelength) of the twin photons. It derives from two effects that participate in the relaxation of the phase matching condition. On the one side the finite transverse dimension of the gain area, coinciding with the pump radius w_p at low parametric gain. On the other side the finite longitudinal dimension of the system, i.e. along the pump propagation direction, that is generally given by the crystal length l . If the first dominates, the coherence area is related to the Fourier transform of the pump transverse profile, i.e. $x_{coh} \propto 1/w_p$. If the second dominates, the coherence area is of the order of $(l \cdot \vartheta)^{-1}$ for small emission angle. The appearance of the emission is a speckled structure in which the speckles have, roughly, the dimension of the coherent area and for any speckle at position \mathbf{q} there exists a symmetrical one in $-\mathbf{q}$ with equal intensity. This is rather evident in the ccd image of SPDC shown in Fig. 1.

Omitting some unessential constants, the Hamiltonian describing the three fields parametric interaction is

$$\widehat{H}_I(t) \propto \int_{\mathcal{V}} \chi^{(2)} \widehat{\mathbf{E}}_1^{(+)}(\mathbf{r}, t) \widehat{\mathbf{E}}_2^{(+)}(\mathbf{r}, t) \widehat{\mathbf{E}}_p^{(-)}(\mathbf{r}, t) d^3r + h.c \quad (1)$$

The pump depletion due to the down-conversion and the absorption is indeed of small entity, unless extremely high intensity laser sources are used. We shall therefore work in the parametric approximation, that treats the pump as a classical monochromatic field propagating linearly along a certain z direction inside the crystal and having an amplitude transverse profile $A_p(\rho)$, i.e.

$$\mathbf{E}_p(\mathbf{r}, t) \propto A_p(\rho) e^{-i(k_p z - \omega_p t)}, \quad (2)$$

where ρ is the coordinate vector in the transverse plane to the propagation direction z .

The down-converted fields 1 and 2 are quantized. Their positive- and negative-frequency part $\widehat{\mathbf{E}}^{(+)}(\mathbf{r}, t)$ and $\widehat{\mathbf{E}}^{(-)}(\mathbf{r}, t)$ is given as an expansion in plane-wave modes and we find convenient to express them separating the sum over the wave-vector into the sum over its transverse component \mathbf{q} and the frequency ω . Thus, we have

$$\widehat{\mathbf{E}}_i^{(+)}(\mathbf{r}, t) \propto \sum_{\mathbf{q}_i, \omega_i} e^{i(k_{iz} z - \omega_i t)} e^{i\mathbf{q}_i \cdot \rho} \widehat{a}_i(\mathbf{q}_i, \omega_i) \quad (3)$$

where $i = 1, 2$. The third component k_{iz} of the i -th field wave vector is expressed in terms of the \mathbf{q}_i and ω_i because of the relations

$$k_{iz} = \sqrt{k_i^2 - q^2} \quad \text{and} \quad k_i = \frac{\omega_i n_i}{c} \quad (4)$$

Introducing Eq.s (2) and (3) in the Hamiltonian (1) we have

$$\begin{aligned} \widehat{H}_I \propto \sum_{\mathbf{q}_1, \omega_1} \sum_{\mathbf{q}_2, \omega_2} \chi^{(2)} \int_0^l e^{i(k_{1z} + k_{2z} - k_p)z} dz \int_{l_x \times l_y} d\rho A_p(\rho) e^{i(\mathbf{q}_1 + \mathbf{q}_2) \cdot \rho} \\ e^{i(\omega_p - \omega_1 - \omega_2)t} \widehat{a}_1(\mathbf{q}_1, \omega_1) \widehat{a}_2(\mathbf{q}_2, \omega_2) + h.c. \end{aligned} \quad (5)$$

Here l is the length of the crystal, while $l_x \times l_y$ is the area of its transverse surface.

The integral in dz gives a contribution proportional to $l \cdot \text{sinc}[(\Delta k l)/2]$ where $\Delta k \equiv k_{1z} + k_{2z} - k_p$. The double integral on the transverse surface of the crystal gives the Fourier transform of the pump transverse profile if the crystal is large compared to it. Supposing a gaussian pump $A_p(\rho) = A_p e^{-\rho^2/w_p^2}$ the Hamiltonian (5) becomes

$$\begin{aligned} \widehat{H}_I \propto \sum_{\mathbf{q}_1, \omega_1} \sum_{\mathbf{q}_2, \omega_2} g \cdot \text{sinc} \left[\frac{\Delta k(\mathbf{q}_1, \mathbf{q}_2, \omega_1, \omega_2) \cdot l}{2} \right] e^{-(\mathbf{q}_1 + \mathbf{q}_2)^2 \frac{w_p^2}{4}} \\ e^{i(\omega_p - \omega_1 - \omega_2)t} \widehat{a}_1(\mathbf{q}, \omega_1) \widehat{a}_2(-\mathbf{q}, \omega_2) + h.c. \end{aligned} \quad (6)$$

where we have introduced the dimensionless factor $g \propto \chi^{(2)} \cdot l \cdot A_p$, usually referred to as parametric gain. Its value determines the number of photons that

are generated in the down conversion process in mode pairs that are well-phase matched. The evolution of the quantum system guided by Hamiltonian (6), in the case of relatively high gain regime, requires a numerical solution and it is discussed in detail in (lug). Anyway, in the first order of the perturbation theory ($g \ll 1$), the quantum state of the scattered light has the entangled form

$$\begin{aligned} |\psi\rangle &= |\text{vac}\rangle + \exp\left[-\frac{i}{\hbar} \int \hat{H}_I dt\right] |0\rangle \\ &= |\text{vac}\rangle + \sum_{\mathbf{q}_1, \mathbf{q}_2} \sum_{\omega_\Omega} F(\mathbf{q}_1, \mathbf{q}_2, \Omega) |1_{\mathbf{q}_1, \Omega}\rangle |1_{\mathbf{q}_2, -\Omega}\rangle, \end{aligned} \quad (7)$$

$$\begin{aligned} F(\mathbf{q}_1, \mathbf{q}_2, \Omega) &= g \cdot \text{sinc}\left[\frac{\Delta k(\mathbf{q}_1, \mathbf{q}_2, \Omega) \cdot l}{2}\right] e^{-(\mathbf{q}_1 + \mathbf{q}_2)^2 \frac{w_p^2}{4}}, \\ \omega_1 &= \omega_p/2 + \Omega, \quad \omega_2 = \omega_p/2 - \Omega. \end{aligned} \quad (8)$$

The coherence area, in the limit of low parametric gain g , can be estimated by the angular structure of the coincidence probability $|F(\mathbf{q}_1, \mathbf{q}_2)|^2$ at some fixed frequency Ω . As mentioned before, now is clear that we deal with two functions that enter in the shaping of the coherence area: the *sinc* function and the Fourier transformed of the gaussian pump profile. Since they are multiplied, the narrower determines the dimension of the area. By expanding linearly the longitudinal wave detuning around the exact matching point $\Delta k(\mathbf{q}_0, \mathbf{q}_0, \Omega)$ according to relations (4), the *sinc* function turns out to have a Half Width Half Maximum of $\Delta q = 2,78/(l \tan \vartheta)$. The HWHM of the gaussian function, appearing in (8), is $\delta q = \sqrt{2 \ln(2)}/w_p$. Concerning our experiment, we consider so small emission angles ϑ and large enough pump radius w_p , that we always work in the region $\delta q/\Delta q < 1$. Therefore, in principle, the dimension of the coherence area is only determined by the pump waist.

When moving to higher gain regime, the number of photon pairs generated in the single mode increases exponentially as $\propto \sinh^2(g)$ i.e. a large number of photons is emitted in the coherence time along the direction ϑ . In this case, also the pump amplitude becomes important in the determination of the speckles dimension. As described in (lug2), this can be explained by a qualitative argumentation: inside the crystal, the cascading effect that causes the exponential growth of the number of generated photons is enhanced in the region where the pump field takes its highest value, i.e. close to the center of the beam. Thus, in high gain regime, most of the photon pairs are produced where the pump field is closed to its peak value. As a result the effective region of amplification inside the crystal becomes narrower than the beam profile. Thus, in the far field one should consider the speckles as the Fourier transform of the effective gain profile, that being narrower, produces larger speckles.

A further fundamental consideration for the practical implementation is that in high gain regime, instead of measuring the coincidences between two photons by means of two single photo-detectors, one collects a large portion of the emission by using for instance a CCD array with a certain fixed exposure time. Within this time several photons are collected by the single pixels and the result is an intensity pattern, having the spatial resolution of the pixel. The coherence area can be evaluated by the cross-correlation between the signal's and the idler's intensity patterns. We can define also the auto-correlation function of the signal intensity

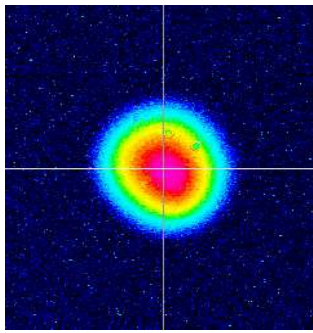


Figure 2. CCD image of the pump beam after spatial filtering.

pattern itself, since in the single transverse mode of the signal arm there are many photons. To be precise the speckle's dimension is better related to the spread of this function, although the two functions, the cross- and the auto- correlation, present the same behaviour with respect to the pump parameters, see (*lug*). From the experimental view-point it is convenient to study the auto-correlation because of the higher visibility that allows a more accurate estimation of its size.

3. Experiment

Our setup is depicted in Fig. 3. A type II BBO non-linear crystal ($l = 1$ cm) is pumped by the third harmonic (wavelength of 355 nm) of a Q-switched Nd:Yag laser. The pulses have a duration of 5ns with a repetition rate of 10 Hz and a maximum energy, at the selected wavelength, of about 200 mJ. The pump beam crosses a spatial filter (a lens with $f=50$ cm and an iris of 250 μm of diameter), in order to eliminate the non-gaussian components (see fig. 2) and to collimate it before the crystal. The diameter of the pump beam entering the crystal is varied, when necessary, by changing the distance between two lenses (a biconvex and a biconcave) placed after the spatial filter. After the crystal, the pump is stopped by a UV mirror, transparent to the visible, and by a low frequency-pass filter. The down converted photons (signal and idler) pass through a lens of 5 cm of diameter ($f = 10$ cm) and an interference filter centered at the degeneracy $\lambda=710$ nm (10nm bandwidth) and finally measured by a CCD camera. We used a 1340X400 CCD array, Princeton Pixis:400BR (pixel size of 20 μm), with high quantum efficiency (80%) and low noise (5 electrons/pixel). The far field is observed at the focal plane of the lens in a $f - f$ optical configuration, that ensures that we image the Fourier transform of the crystal exit surface. Therefore a single transverse wavevector \mathbf{q} is associated to a single point $\mathbf{x} = (\lambda f/2\pi)\mathbf{q}$ in the detection plane. The CCD acquisition time is set to 90 ms, so that each frame corresponds to the PDC generated by a single shot of the laser.

Looking at the images, we can appreciate the speckled structure and a certain level of correlation of the speckles intensity between the signal and idler arms (Fig. 4). Let us define $N_R(\mathbf{x})$ the intensity level, proportional to the number of photons, registered by the pixel in the position \mathbf{x} of the region R . $\delta N_R(\mathbf{x}) = N_R(\mathbf{x}) - \langle N_R(\mathbf{x}) \rangle$ is the fluctuation around the mean value that is estimated as $\langle N_R(\mathbf{x}) \rangle = (1/n) \sum_{\mathbf{x}} N_R(\mathbf{x})$, with n the number of pixels. We evaluate the normalized spatial cross-correlations of the intensity fluctuations in an arbitrary region R_1 , belonging to the signal portion of the image, and in the symmetric region R_2 (see Fig. 4) belonging to the idler portion:

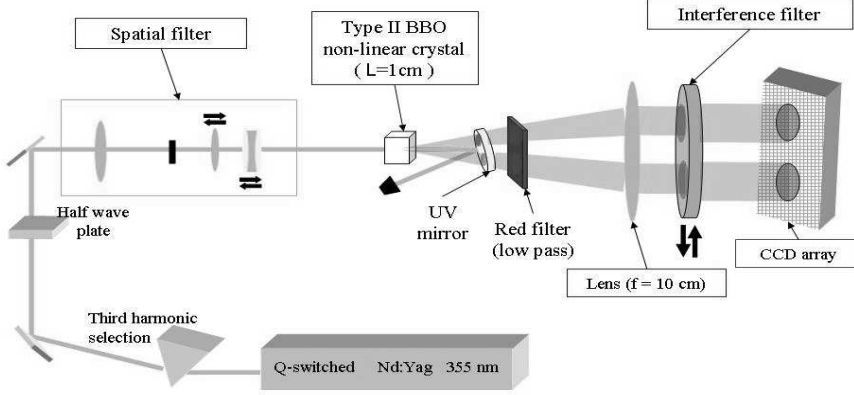


Figure 3. Experimental setup. A triplicated Nd-Yag laser beam, after spatial filtering, produces type II PDC in a BBO crystal, which is then measured, after an interference filter and pump elimination, by a CCD camera.

$$C_{12}(\xi) = \frac{\langle \delta N_{R_1}(\mathbf{x}) \delta N_{R_2}(-\mathbf{x} + \xi) \rangle}{\sqrt{\langle \delta N_{R_1}(\mathbf{x})^2 \rangle \langle \delta N_{R_2}(-\mathbf{x} + \xi)^2 \rangle}} \quad (9)$$

where ξ is the displacement vector that assumes discrete values. C_{12} reaches a peak of about 0,9 in Fig. 4-a, that indicates a good level of spatial correlation between signal and idler. In figure 4-b the value is around 0,6 because here we did not put the interference filter in front of the CCD camera, allowing more background light to enter, and the signal and idler component are not separated. It is worth to emphasize that $C_{12}(\xi)$ is not a index of the correlation at the quantum level and it can not be used to discriminate the SSN condition. We are interested mainly in the width of the peak, that indicate the coherence area.

Since the experimental cross-correlation is characterized by a non-optimal visibility, due to the losses in optical paths and noise, we preferred to estimate the speckle's size, by evaluating the auto-correlation of a single region R of the signal intensity pattern.

$$C(\xi) = \frac{\langle \delta N_R(\mathbf{x}) \delta N_R(\mathbf{x} + \xi) \rangle}{\sqrt{\langle \delta N_R(\mathbf{x})^2 \rangle \langle \delta N_R(\mathbf{x} + \xi)^2 \rangle}}. \quad (10)$$

First off all we investigate the gain region in which we are working, in order to ensure the possibility to reach a sufficient non-linear cascading effect in the photon pairs production inside the crystal. Fig. 5 shows the mean photon number $\langle N_R(\mathbf{x}) \rangle$ as function of the pump power PW . Any point is averaged over several tenths of frames in order to reduce the uncertainty. Our laser presents in fact 20% fluctuations of the power from pulse-to-pulse. Since the mean number of photons is proportional to $\sinh^2(g)$, the fluctuations of the pump generate large fluctuations in the photons number from frame-to-frame. The diameter of the pump is fixed and the power is varied by the delay between the Q-switch turn-on and the lamp

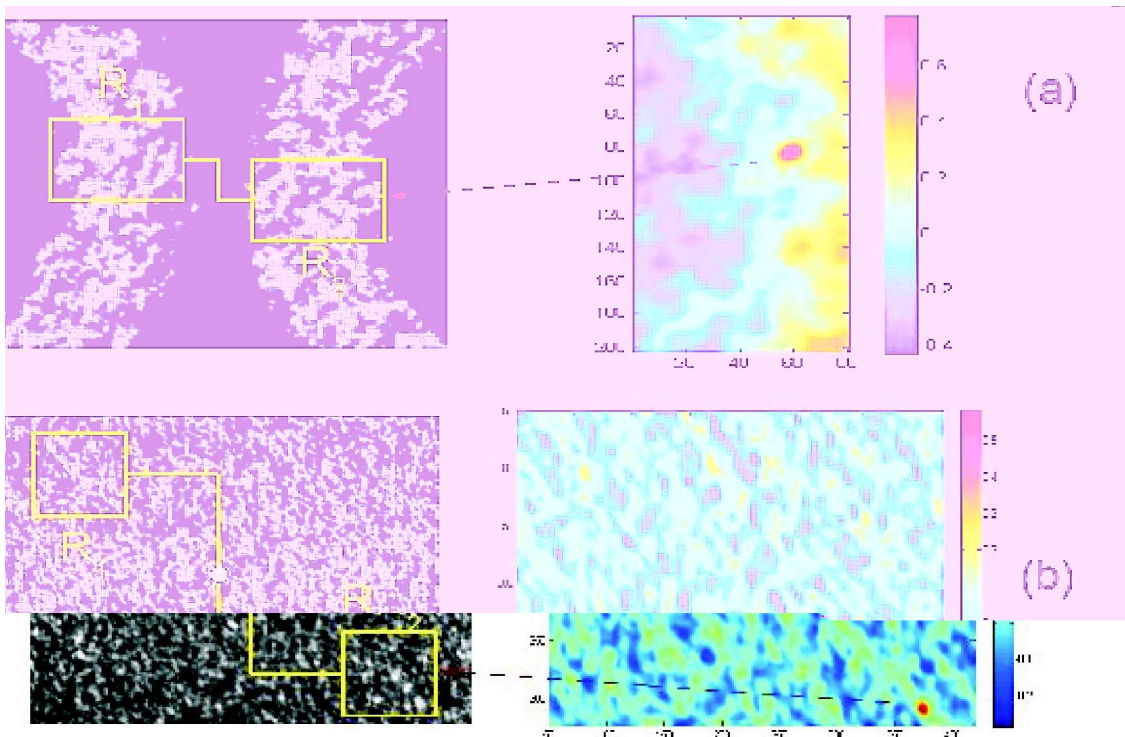


Figure 4. Spatial correlation between signal and idler down converted light with interference filter around degeneracy(a) and without a narrow filter (b). In each row the first inset is a ccd image, the second a plot of the cross correlation function. The axis report the pixels position in the CCD array. $C_{12}(\xi)$.

flash. The calibration curve delay-power has been measured by a power meter and we observed a reproducibility with uncertainty around 10%.

In Fig. 5-a the pump diameter is around 1,3mm and in Fig. 5-b is 0,95mm. Although the pump power used for the case (b) is smaller than case (a), the intensity results higher in the case (b) because of the reduced radial dimension. It must be noticed that we are constrained in the range of intensities of the pump. For high intensities we are limited by the damage threshold of optical components, for low intensities by the visibility of the speckle structure because we collect a lot of temporal modes in the same frames.

The data are fitted by the equation $\langle N_R \rangle = k \cdot \sinh^2(\sigma\sqrt{p})$. k depends from the number of modes while $\sigma\sqrt{P} = g$. The experimental values, mediated on three different acquisitions, are $k = 31.48$ and $\sigma = 1.91$ for the case (a). In the case (b) we obtain $k = 1,10$ and $\sigma = 4,87$; the higher value of σ is due to the increased intensity. Therefore, in the case (a) we have a gain g from 1,5 to 3,5 and in the case (b) from 1,9 to 5. Thus, we are in a non-linear regime where we should expect a dependence of the speckles size from the amplitude of the pump.

Fig. 5-c and 5-d show the trend of the radius of the coherence area with the pump power, again at the two different diameters of the pump. Actually we observe an increasing of the radius, that is predicted by the considerations exposed in section 2. We consider, just as indicative, a linear fit $y = a(x - b)$, obtaining $a = 1,25$ and $b = -0,63$ for (c) and $a = 3.7$ and $b = -0,27$ for (d). The higher slope of (c) is qualitatively explained by the higher gain.

Finally, we investigate the dependence of the radius of the speckles from the pump diameter, as shown in figure 6. We fix the power of the laser to 0,78 MW and we change the diameter varying the distance between the two collimating lenses (see figure 3). The two curves differ just in the estimation of the pump diameter:

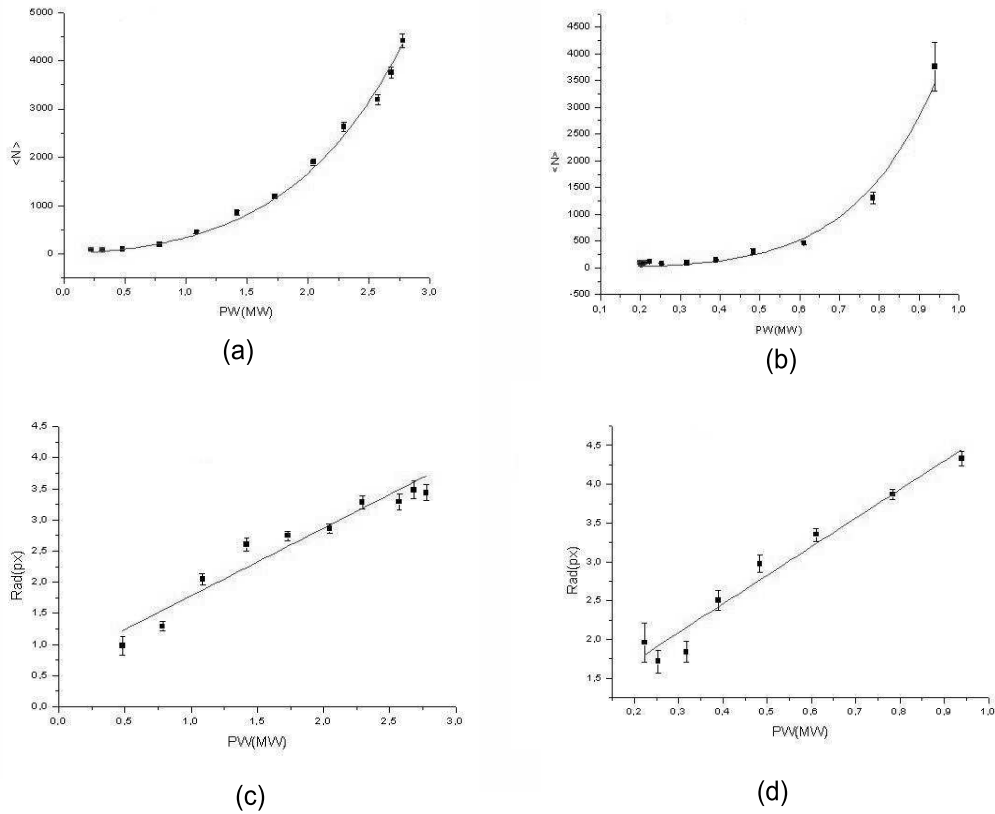


Figure 5. The top of the figure represents the mean number of photon/pixel collected by the CCD in one shot of the laser (5ns), function of the pump pulse power in MW. The bottom represents the dependence of the speckle radius (in pixel) from the pump power. In (a) and (c) the pump diameter is 1,3mm, while in (b) and (d) is 0.95mm.

in one case we measured it with an impact paper (IP) and in the other case with a CCD. We perform a fit in the form $y = a \cdot x^b$ obtaining $a = (8,1 \pm 0,1)$ and $b = (-3,61 \pm 0,09)$ for the IP curve and $a = (3,22 \pm 0,07)$ and $b = (-3,73 \pm 0,09)$ for the CCD curve. Despite the different way of pump size estimation, reflected in the value of the parameter a , the coefficients b are compatible. The theory, in low gain regime, provides that the radius of the speckles is proportional to the inverse of the pump size (w_p), i.e. $b = -1$. The estimated value of b , in our case, confirms the role of the high gain regime in the speckle size. In fact, together with the reduction of the pump diameter, the gain increases, and thus the effective gain area is more reduced again. This effect impresses upon the speckles size a stronger dependence with respect to the pump size.

4. Conclusion

This paper provides a detailed experimental study of the size of the coherence area in PDC in the high gain regime. We show that the speckles present, not only a dependence on the pump diameter, as in the usual low gain regime, but also a strong dependence from the pump intensity. The understanding of the behaviour of the coherence area in the high gain regime is fundamental for the innovative application in the field of quantum imaging. In general, these results allow the

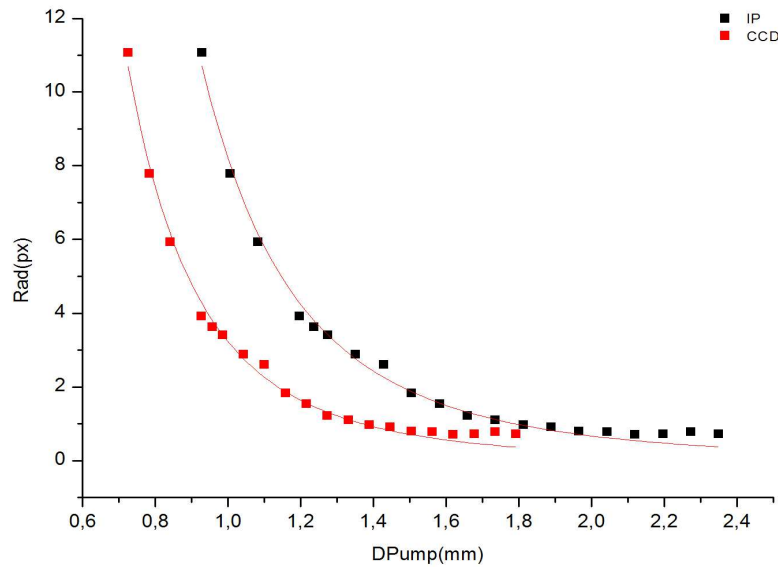


Figure 6. Observed dependence of the radius (in pixels) of the speckles from the pump diameter. The two curves differs in the estimation of the pump diameter: in one case it was measured with an impact paper (IP) and in the other case with a CCD.

tailoring of speckles properties, an instrument useful not only for applications to quantum imaging but also for quantum metrology, quantum information, etc.

4.1. Acknowledgments

This work has been supported by MIUR (PRIN 2005023443-002), by 07-02-91581-ASP and by Regione Piemonte (E14). Thanks are due to Alessandra Gatti, Ottavia Jedrkiewicz and Luigi Lugiato for useful discussions.

References

- (las) Goodman, J.W., *Laser speckle and Related Phenomena* ; Springer Verlag: Berlin, 1984.
- (uto) Uno, K. et al., *Opt. Comm.* **1996**, *124* 16; Uozumi, J. et al. *Opt. Comm.* **1998**, *156* 350; Funamizu, H., Uozumi, J., *Journ. Mod. Opt.* **2007**, *54* 1511;
- (qi) Kolobov, M.I. editor *Quantum Imaging* ; Springer Verlag: Singapore.
- (lug) Brambilla, E. et al., *Phys. Rev. A* **2004**, *69* , 023802-1 –6; *Eur. Phys. J. D* **2001**, *15* 117.
- (mat) A. allevi et al., *Las. Phys.* **2006**, *16* , 1451.
- (dit) Jedrkiewicz, O. et al., *Phys. Rev. Lett.* **2004**, *93* , 243601-1 –4; *Journal of Modern Optics* **2006**, *53*, 575-595
- (lug2) Brambilla, E. et al., arXiv:0710.0053
- (and) Bondani, M. et al., *Phys. Rev. A* **2007**, *76* , 013833
- (1) Genovese, M. *Physics Reports*, **2005**, 413/6.